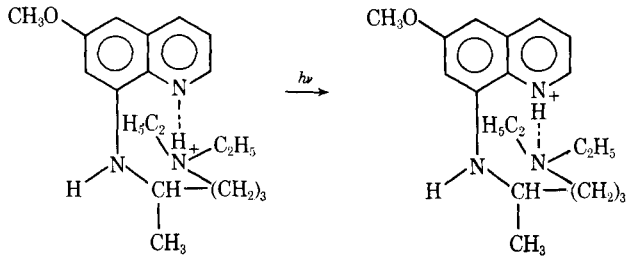

Scheme V

group, excitation of the singly protonated species would result in transfer of the proton, across the intramolecular hydrogen bridge, from the diethylamino group to the ring nitrogen. Presumably, in the thermally equilibrated excited state, the proton would be covalently bonded to the ring nitrogen and electrostatically hydrogen bonded to the diethylamino group (Scheme V).

Thus the excited singly protonated species would have an electronic distribution similar to that of the doubly protonated species in the aromatic ring, and this would account for the similarity of emission frequency between the singly and doubly protonated species. That the emission frequency of the singly protonated species is slightly higher than that of the doubly protonated species in *n*-heptane can be explained by the intramolecular hydrogen bond with the diethylamino group which partially withdraws the proton from the ring nitrogen atoms, thus diminishing its polarizing effect on the π-electron distribution of the aromatic system. The intramolecular hydrogen bond with the diethylamino group in the excited state also serves to shield the proton of the excited singly protonated species from the solvent. This accounts for the observation of fluorescence from the singly protonated species of pamaquine but not from the doubly protonated pamaquine or singly protonated 8-amino-6-methoxyquinoline, both of which have similar electronic structures to that of the singly protonated pamaquine.

The fluorometric titration of pamaquine near pH 14 can be attributed to protolytic dissociation, in the excited state, from the heterocyclic nitrogen atom of singly protonated pamaquine. The pKa* corresponding to this dissociation is 14.0. This dissociation occurs at such high pH because of the increase in basicity of the ring nitrogen upon excitation and supports the hypothesis of protonation of the ring nitrogen in the excited state of singly protonated pamaquine. That the fluorescence of the free base pamaquine occurs at substantially lower frequencies than in *n*-heptane is probably the result of electrostatic stabilization of the excited state of the free base by dipole–dipole interactions with the highly polar aqueous solvent. That pamaquine fluoresces as the free base in aqueous solutions while 8-amino-6-methoxyquinoline does not appears to be the result of protection of the ring nitrogen atom of pamaquine from hydrogen-bonding interactions with the solvent. Although dissociation removes the hydrogen bond between the alkyl side chain and the ring nitrogen atom, the time required for the chain to become disoriented from the ring nitrogen atom may be slow compared with the lifetime of the excited state of pamaquine, so the chain may provide a steric blockage to approach of solvent molecules which would quench the fluorescence of the excited free base.

REFERENCES

(1) B. B. Brodie, S. Udenfriend, and J. V. Taggart, *J. Biol. Chem.*, **168,** 327(1947).

(2) J. L. Irvin and E. M. Irvin, *ibid.*, **174,** 577(1948).

(3) S. Udenfriend, D. E. Duggan, B. M. Vasta, and B. B. Brodie, *J. Pharmacol. Exp. Ther.*, **120,** 26(1957).

(4) S. G. Schulman and L. B. Sanders, *Anal. Chim. Acta*, **56,** 91(1971).

(5) M. J. Jorgenson and D. R. Hartter, *J. Amer. Chem. Soc.*, **85,** 878(1963).

(6) S. R. Christophers and J. D. Fulton, *Ann. Trop. Med. Parasitol.*, **34,** 1(1940).

(7) A. Weller, *Progr. React. Kinet.*, **1,** 85(1971).

(8) S. G. Schulman, *J. Pharm. Sci.*, **60,** 371(1971).

(9) S. G. Schulman, *Rev. Anal. Chem.*, **1,** 85(1971).

(10) S. G. Schulman and A. C. Capomacchia, *Anal. Chim. Acta*, **58,** 91(1972).

ACKNOWLEDGMENTS AND ADDRESSES

Received January 10, 1972, from the *College of Pharmacy, University of Florida, Gainesville, FL 32601*

Accepted for publication May 25, 1972.

The authors are grateful to Dr. S. Archer of the Sterling-Winthrop Research Institute, Rensselaer, N. Y., for providing a sample of pamaquine phosphate.

▲ To whom inquiries should be directed.

Kinetics of Solvolysis of Intrazole

V. K. PRASAD, R. A. RICCI, and A. P. GRANATEK▲

Abstract □ The kinetics of degradation of intrazole [1-(*p*-chlorobenzoyl)-3-(1*H*-tetrazol-5-ylmethyl)indole] in solution was investigated at 65 ± 0.1° at constant ionic strength of 0.5 over a wide pH range. The observed rates, followed by measuring intact intrazole, obeyed first-order kinetics. The catalytic effect of a phosphate buffer was found to be greater than the acetic acid catalysis. The apparent rate of hydrolysis of intrazole increased with the increasing concentration of hydrochloric acid. Primary salt effects were observed in both acidic and basic solutions. The rate of hydrolysis decreased in acidic and alkaline solutions, with increasing concentrations of ethanol in the solvent system. The apparent heats of activation for intrazole degradation in solution were determined to be 19.87 kcal./mole in 0.1 *N* HCl, 21.40 kcal./mole in pH 4.10 acetate buffer, 20.30 kcal./mole in pH 8.0 phosphate buffer, and 7.25 kcal./mole in pH 9.10 and 10.10 borate buffers. From the rate–pH profile, the pH of minimum degradation or maximum stability of the compound under buffer-free conditions was found to be 3.20. The products of hydrolysis formed in acid- and alkali-catalyzed degradation of intrazole were identified by TLC. A mechanism consistent with the above observations is proposed.

Keyphrases □ Intrazole—solvolysis, pH–rate profile □ pH–solvolysis rate profile—intrazole

The anti-inflammatory, antipyretic, and analgesic properties of intrazole (I), the most effective member of a series of 1-substituted 3-(5-tetrazolylmethyl)indoles, were described by Fleming *et al.* (1). It was shown to be equally active in intact and adrenalectomized rats as an anti-inflammatory agent (carrageenin foot edema assay).

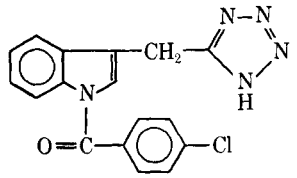

I

It also potentiated the antiphlogistic activity of hydrocortisone in the granuloma pouch and effectively prevented or alleviated adjunct-induced polyarthritis. The major advantage of this compound appears to be its low level of toxicity. It exhibited a larger effective dose–toxic dose ratio than other available anti-inflammatory agents in both single- and multiple-dose studies. The synthesis of intrazole and related compounds was reported by Juby and Hudyma (2).

This paper describes the solvolysis of intrazole in various buffers and presents the rate–pH profile, Arrhenius parameters, and other related information valuable in the formulation of dosage forms of this compound. Intrazole solvolysis is interesting in that the amide linkage is part of the heterocyclic system and the mechanism of degradation could be different in comparison to the classical amides.

Normal amides are characterized by relatively low reactivity in nucleophilic reactions (*e.g.*, hydrolysis or alcoholysis). However, Staab (3, 4) used the term reactive heterocyclic amides or "azolides" to describe amides whose amide nitrogen is a member of a quasi-aromatic five-membered ring containing at least two nitrogen atoms, *i.e.*, azoles. During his investigations, he found that the high degree of reactivity of azolides and the order of reactivity in this group are related to the quasiaromatic character of azoles. However, in the indole series, Staab (4) found that the order of reactivity, *i.e.*, rate of hydrolysis, in conductivity water at 25° at pH 7.0 increased with the number of nitrogen atoms in the ring (II, III, and IV). The complete inertness of II could be due to the inactivity of the ring nitrogen and the electron-donating nature of the methyl group. Therefore, it seemed logical to investigate the hydrolysis of intrazole, where the methyl group has been replaced with the more reactive electron-attracting *p*-chlorobenzoyl group.

EXPERIMENTAL[1]

Materials—Intrazole was recrystallized from chloroform (m.p. 233–234°). Distilled water, boiled and purged with nitrogen while cooling, was used to prepare the buffers. The buffers used were: pH <3.0, HCl–KCl; pH 3.0–5.60, sodium acetate–acetic acid; pH 5.60–8.0, Na_2HPO_4–NaH_2PO_4; and pH >8.0, borate. These buffers were prepared according to the procedure described by Dawson and Elliott (5).

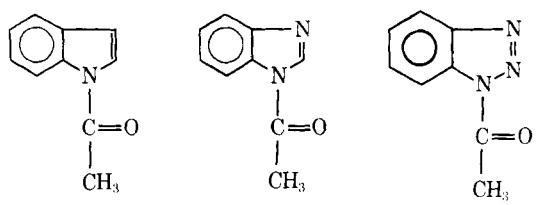

II III IV

Determination of pKa of Intrazole—A stock solution of intrazole in anhydrous ethanol (2 mg./ml.) was prepared. Exactly 5 ml. of this stock solution was transferred to a 50-ml. beaker, and the required volume of nitrogen-purged distilled water and the calculated volume of anhydrous ethanol were added so that the concentration of ethanol in the final solution varied from 50 to 80% (by volume). Nitrogen, which had been passed through distilled water at room temperature, was bubbled through this solution while titration with 0.01 *N* alcoholic potassium hydroxide was carried out using the dual recording titrator. From the titration curve, the pKa was determined in the usual manner.

Kinetic Measurement—In a typical kinetic run, 1 ml. of a 0.01 *M* (0.3375 g./100 ml.) stock solution of intrazole in 95% ethanol was added to 7.0 ml. of ethanol and diluted to 100 ml. with thermally equilibrated buffer. Approximately 4.0 ml. of the sample was withdrawn at intervals and cooled to room temperature; readings were taken on either of the two spectrophotometers used[2]. The pH of the buffers, before and after the kinetic run, were determined at the temperature of the study.

TLC—*Acid-Catalyzed Degradation Products of Intrazole*—A 0.01 *M* solution of intrazole was made in a sufficient volume of ethanol and 0.1 *N* hydrochloric acid and heated at 65°. At regular intervals, a small sample was diluted to 10^{-4} *M*, and the absorbance at 306 nm. was determined. When the absorbance of the diluted solution reached an asymptote value (0.050 absorbance unit), heating was stopped and the solution was cooled and extracted several times with chloroform. The chloroform extracts were dried over anhydrous sodium sulfate and evaporated *in vacuo*. The residue was redissolved in ethanol so that the final concentration of the solution was 0.01 *M*. Five microliters of this solution was spotted on silica gel F_{254} plates[3]. Reference compounds of intrazole, *p*-chlorobenzoic acid, and 3-(5-tetrazolylmethyl)indole with the same concentration as the degraded material were also spotted. The plate was developed in a solvent system consisting of benzene–methanol–glacial acetic acid (70:10:1). The R_f values were: *p*-chlorobenzoic acid, 0.56; intrazole, 0.43; and 3-(5-tetrazolylmethyl)indole, 0.28. The products of acid hydrolysis of intrazole were found to be *p*-chlorobenzoic acid, 3-(5-tetrazolylmethyl)indole, and another minor product with the same R_f as intrazole.

Since it was evident from the spectral absorbance of the solution that the latter material was not intrazole, and since *p*-chlorobenzoic acid was one of the degradation products, it could be a derivative of 3-(5-tetrazolylmethyl)indole. To verify this, an alcoholic solution of 3-(5-tetrazolylmethyl)indole (0.01 *M* in 0.1 *N* HCl) was heated at 65° for the same period as intrazole was heated. The solution was diluted with distilled water and extracted several times with chloroform. The chloroform extracts were combined and washed twice with cold distilled water, dried over anhydrous sodium sulfate, and filtered, and the chloroform was removed under vacuum. The residue was dissolved in ethanol to produce a 0.01 *M* solution and then chromatographed as described earlier along with reference compounds and acid-catalyzed hydrolytic products of intrazole, using the same developing system. The unidentified product resulting from the acid-catalyzed hydrolysis of intrazole had the same R_f value (0.43) as the acid-catalyzed degradation product of 3-(5-tetrazolylmethyl)indole. That the unidentified product was actually the result of further degradation of 3-(5-tetrazolylmethyl)indole, which was a product of the acid hydrolysis of intrazole, was substantiated by this experiment. No significant amount of the unknown product could be detected on the TLC plate when the yield of *p*-chlorobenzoic acid approached the theoretical quantity. Due to the lack of availability of this unknown derivative of 3-(5-tetrazolylmethyl)indole, it was not further characterized.

To quantify the yield of *p*-chlorobenzoic acid from the acid-catalyzed hydrolysis of intrazole, 10 μl. of the ethanolic extract of

[1] A Cary model 15 recording spectrophotometer, Beckman model DU spectrophotometer, Beckman expanded scale pH meter, and Sargent-Welch model DG dual recording titrator were used.

[2] When readings were taken on the Beckman model DU, the decrease in the 306-nm. chromophore due to the degradation of intrazole was followed.

[3] E. Merck, Darmstadt, W. Germany.

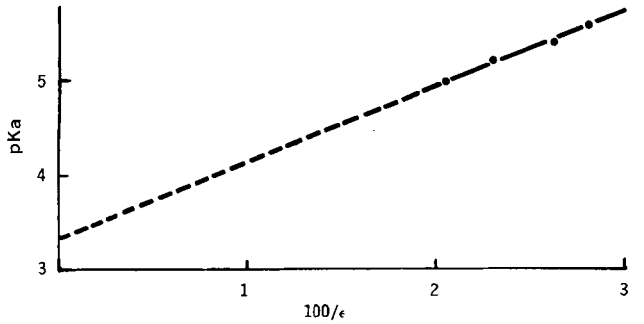

Figure 1—*pK'a of intrazole* versus *100/(dielectric constant) of the solvent medium at 25 ± 0.1°. The pKa of intrazole in pure water is 4.40, corresponding to a 100/dielectric constant value of 1.27.*

the acid-catalyzed hydrolytic solution of intrazole was chromatographed along with a similar quantity of *p*-chlorobenzoic acid in ethanol. The spots were eluted and diluted to 10 ml. with ethanol. One milliliter of this solution was diluted with distilled water, and the absorbance was determined at 240 nm. The amount of *p*-chlorobenzoic acid was calculated from a calibration curve. It was found that the amount of *p*-chlorobenzoic acid resulting from the degradation of intrazole in hydrochloric acid was 92–95% of the theory. The recovery of *p*-chlorobenzoic acid of known concentration was 92–96%.

Products of Hydrolysis of Intrazole in Alkaline Solution—Intrazole, 0.01 *M* solution in 0.10 *N* sodium hydroxide, was heated at 40° for 2 hr. An aliquot was taken at intervals and appropriately diluted, and the absorbance at 306 nm. was determined. When the absorbance approached an asymptotic value, the solution was cooled and its pH was adjusted to 2.0 with concentrated hydrochloric acid. The solution was extracted several times with chloroform, and the procedure was repeated as described under the TLC separation of acid-catalyzed hydrolysis products of intrazole. Only two products accounting for 95% of the theory were observed. One product was 3-(5-tetrazolylmethyl)indole and the other *p*-chlorobenzoic acid. The identity of these products was determined using the same procedure followed for identification of the products of acid hydrolysis.

RESULTS AND DISCUSSION

pKa of Intrazole—Since intrazole has very low aqueous solubility, it could not be titrated in aqueous solution. The spectrophotometric method of determining the pKa was attempted. However, it was found that the absorption maxima of the neutral and dissociated forms of intrazole were nearly identical. Therefore, the method of choice was to determine the pKa in hydroalcoholic mixtures and extrapolate a plot of pKa *versus* percent alcohol to zero alcohol concentration. Since the dielectric constant of the medium is a function of alcohol concentration of the titrating solution, the observed pKa at various alcohol concentrations was plotted against $100/E$, where E is the dielectric of the medium according to Davies (6) (Fig. 1). The pKa value in pure water, the dielectric constant being 78.5 at room temperature (7), was obtained by extrapolation. An average value for pKa from such determinations for intrazole was 4.40. Tetrazole is a weak acid similar in strength to acetic acid (pKa 4.76), and the acidity of the 5-monosubstituted tetrazoles is dependent on the substituent in the 5-position (V) and is increased by electron-withdrawing groups and decreased by electron-releasing groups (8).

Order of Reaction and Observed Rate Constants—Characteristic spectral changes occurring during the degradation of intrazole in the pKa region are shown in Fig. 2. Similar data (well beyond the pKa region) pointed to the fact that no other characteristic chromophores developed during the intrazole degradation. The characteristic absorbance peak at 306 nm. reached asymptote value. The residual absorbance at 306 nm. did not vary significantly with respect to the pH, thereby indicating that the various products of degradation did not interfere at this wavelength.

The apparent first-order rate constants for the degradation of intrazole in various buffers were calculated from slopes of the plots of the logarithms of the difference in the absorbance A_t at any time

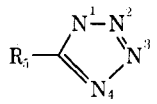

V

t and the final absorbance A_∞ at 306 nm. against time t in accordance with the equation:

$$\log (A_t - A_\infty) = \frac{-kt}{2.303} + \log (A_0 - A_\infty) \qquad \text{(Eq. 1)}$$

where $(A_0 - A_\infty)$ is the absorbance at zero time. Typical first-order plots for the degradation of intrazole in various buffers at 65.0 ± 0.1° are shown in Fig. 3. The observed first-order rate constants and the experimental conditions for the solvolytic degradation of intrazole are given in Tables I and II for the various buffers studied.

General-Acid and General-Base Catalysis—*Acetate Buffers*—It was observed that during the hydrolysis of intrazole, the first-order rate constants increased with increasing concentrations of buffer components. If k_{ACT} is designated as the rate constant for acetate and k^1 is the rate constant for all other factors, then between pH 3.6 and 5.60:

$$k_{obs} = k^1 + k_{ACT}[AC]_T \qquad \text{(Eq. 2)}$$

where $[AC]_T$ is the total concentration of the buffer. Thus, a plot of k_{obs} *versus* $[AC]_T$ produced a straight line with slope k_{ACT} and intercept k^1. Since the species present in acetate buffers in the pH 3.60–5.60 range are HAC and AC^-, one may write:

$$k_{ACT}[AC]_T = k_2[HAC] + k_3[AC^-] \qquad \text{(Eq. 3)}$$

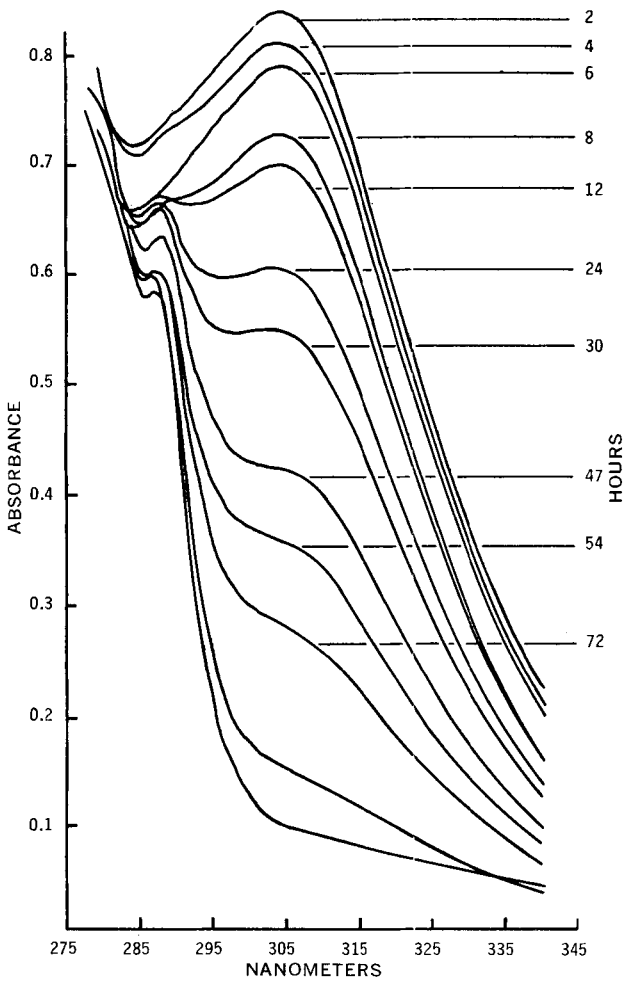

Figure 2—*UV curves for the hydrolysis of intrazole (10^{-4} M) in pH 4.10 acetate buffer ($\mu = 0.5$) at 85.0 ± 0.1° at various times.*

Table I—Observed First-Order Rate Constants Resulting from the Degradation of Intrazole (10^{-4} *M*) in Acetic Acid-Sodium Acetate Buffers at 65.0 ± 0.1° and Ionic Strength 0.5 (KCl)

pH	Observed Rate Constant × 10^3 hr.$^{-1}$ at Total Buffer Concentration, moles/l. 0.05	0.075	0.10	0.15	0.20	Slope	k_0[a]
3.60	2.49	2.59	2.75	2.95	3.22	0.0048	2.30
4.00	3.75	3.95	4.12	4.57	4.90	0.0078	3.40
4.40	4.44	4.79	5.09	5.52	5.85	0.0092	4.00
4.80	5.50	5.93	6.15	6.82	7.45	0.0128	4.80
5.20	6.10	6.53	6.85	7.60	8.38	0.0150	5.40
5.60	9.70	10.0	10.80	11.50	13.10	0.0223	9.00

[a] k_0 is the extrapolated rate constant and represents the rate under buffer-free conditions.

Table II—Observed First-Order Rate Constants Resulting from the Degradation of Intrazole (10^{-4} *M*) in Phosphate Buffers at 65.0 ± 0.1° and Ionic Strength 0.5 (KCl)

pH	Observed Rate Constant × 10^2 hr.$^{-1}$ at Total Buffer Concentration, moles/l. 0.05	0.075	0.10	0.15	0.20	Slope	k_0[a]
6.00	1.32	1.45	1.56	1.74	1.97	0.042	1.15
6.45	2.15	—	2.47	2.90	3.10	0.063	1.84
6.95	6.34	6.65	7.05	7.40	8.10	0.13	5.70
7.20	10.50	11.10	11.60	12.30	13.00	0.16	9.90
7.60	26.90	27.20	27.90	28.90	30.10	0.20	25.9
7.90	54.50	57.00	57.50	60.15	62.50	0.22	53.3

[a] k_0 is the extrapolated first-order rate constant and represents the rate under buffer-free conditions.

where k_2 and k_2 are now the rate constants due to acetic acid and acetate-ion catalysis, respectively. Dividing through by AC_T results in Eq. 4:

$$k_{AC_T} = k_2 f_{HAC} + k_3 f_{AC} \qquad \text{(Eq. 4)}$$

where f_{HAC} and f_{AC^-} are the fractions of acetic acid and acetate ion, respectively, at the particular pH. Since $f_{HAC} + f_{AC^-} = 1$, a plot of k_{AC_T} *versus* f_{AC^-} should be linear with intercept k_2 when f_{AC^-} equals zero and with intercept k_3 when f_{AC} equals unity. Such a plot is shown in Fig. 4; from this, k_2, the rate constant due to acetic acid catalysis, and k_3, the rate constant due to acetate-ion catalysis, were found to be 5.25×10^{-3} and 1.94×10^{-2} l. mole^{-1} hr.$^{-1}$, respectively. Thus, acetate anion seems to catalyze the hydrolysis of intrazole about 3.7 times more than its conjugate acid. Rate constants of the acetate buffers are given in Table I.

Phosphate Buffer Catalysis—The observed rate constants at pH 6–8 were also shown to be affected by the buffer components. This is clear from the data in Table II. The observed rate constants also were plotted as a function of total phosphate concentration according to Eq. 5:

$$k_{obs} = k_0 + k_{phosphate}[\text{phosphate}] \qquad \text{(Eq. 5)}$$

From the slopes of the lines, $k_{phosphate}$ is determined. Because of the species present in the phosphate buffers in the pH region studied (6.00–8.00), the contribution from $H_2PO_4^-$ and HPO_4^{-2} only is important; then:

$$k_{phosphate} = k_{H_2PO_4^-}[H_2PO_4^-] + k_{HPO_4^{-2}}[HPO_4^{-2}] \qquad \text{(Eq. 6)}$$

$$= k_{H_2PO_4^-} f_{H_2PO_4^-} + k_{HPO_4^{-2}} f_{HPO_4^{-2}} \qquad \text{(Eq. 7)}$$

In Eq. 7, $f_{H_2PO_4^-}$ and $f_{HPO_4^{-2}}$ represent the fractions of monoanion and dianion of phosphoric acid at that particular pH, respectively. Since $f_{H_2PO_4^-} + f_{HPO_4^{-2}} = 1$, a plot of $k_{phosphate}$ *versus* $f_{HPO_4^{-2}}$ should be linear with the intercept $k_{HPO_4^{-2}}$ when $f_{HPO_4^{-2}}$ equals unity. Such a plot is shown in Fig. 5; from this, $k_{HPO_4^{-2}}$, the rate constant due to HPO_4^{-2} ion catalysis, is found to be 2.25×10^{-1}

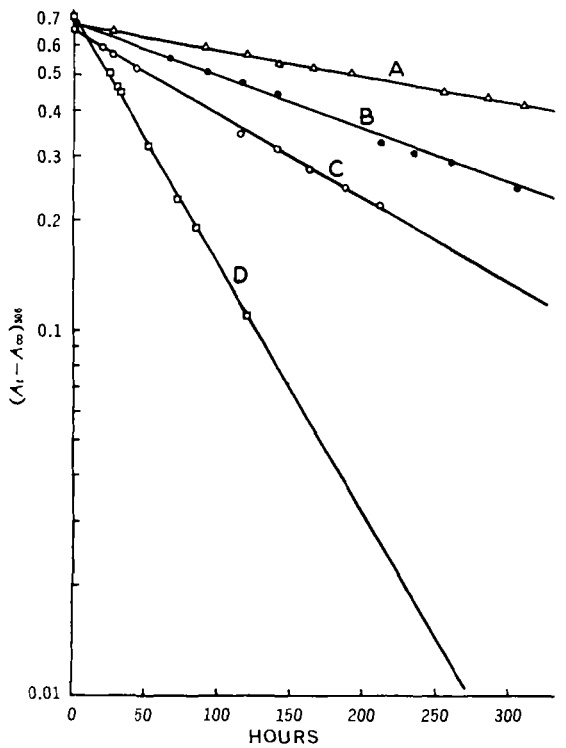

Figure 3 *-Typical first-order plots for the hydrolysis of intrazole (10^{-4} M) in various buffers (μ = 0.5) at 65.0 ± 0.1°. Key: A, pH 3.2; B, pH 4.0; C, pH 5.2; and D, pH 6.0.*

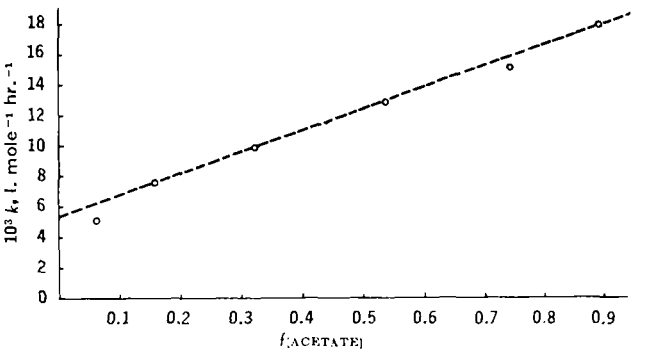

Figure 4—*Plot of rate constant for acetate catalysis* versus *fraction of acetate ion which determined* k_{HAC} *and* k_{AC^-} *for the degradation of intrazole at 65.0 ± 0.1°.*

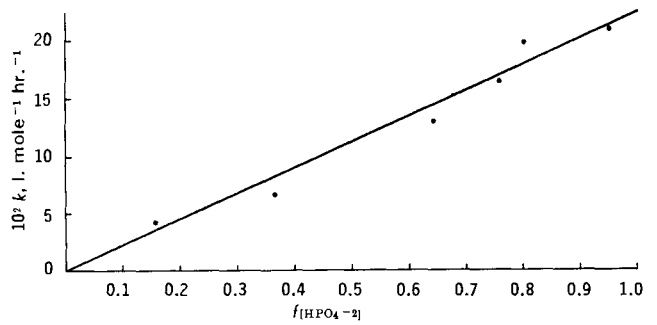

Figure 5—*Plot of rate constant for phosphate-ion catalysis* versus *fraction of* HPO_4^{-2} *which determined* $k_{H_2PO_4^-}$ *and* $k_{HPO_4^{-2}}$ *for the hydrolysis of intrazole at 65°.*

l. mole^{-1} hr.$^{-1}$, and $H_2PO_4^-$ ion does not catalyze the hydrolysis. Borate ion has a negligible catalytic effect on the hydrolysis of intrazole.

Ionic Strength Effects—The rates of degradation of intrazole in 0.1 *N* hydrochloric acid at 65 ± 0.1° were determined at varying salt concentrations. The observed first-order rate constants, k_{obs}, were plotted as a function of the square root of ionic strength according to the equation:

$$\log k_{obs} = \log k + Z_A Z_B A\sqrt{\mu} \qquad \text{(Eq. 8)}$$

where μ is the ionic strength, Z_A and Z_B are the charges on the reacting species, log k is the rate constant in an infinitely dilute solution where $\mu = 0$, and A is a function of the properties of the solution (9). The degradation rate of intrazole was determined in 0.001 *N* sodium hydroxide at 30.0 ± 0.1° and in pH 9.2 borate buffer at 33 ± 0.1° as a function of ionic strength which was adjusted with potassium chloride. Data were plotted according to Eq. 8 (Fig. 6). The positive slope in strongly acidic solutions indicates that the degradation of intrazole involves the attack of a positively charged hydronium ion on a neutral intrazole molecule (10). It is obvious that the ionic strength effect on the rate of hydrolysis of intrazole is not too large, as evidenced by the slope of the line in Fig. 6. However, the slight positive salt effect can be explained according to the modified equation of Debye–Huckel (10) which, in theory, predicts a linear dependence of log k on the ionic strength when a neutral molecule and an ion are involved in the transition state. In alkaline solutions the rate of hydrolysis of intrazole increased as the salt concentration was increased, thus indicating that two negatively charged ions were involved in the transition state.

Dielectric Constants Effects on Solvolysis of Intrazole—To study the effect of the dielectric constant of the medium on the hydrolysis of intrazole, the kinetics of degradation were studied in 0.1 *N* hydrochloric acid (at 65 ± 0.1°) and in 0.003 *N* sodium hydroxide (at 26 ± 0.1°) containing varying amounts of ethanol. The observed first-order rate constants were plotted as a function of $1/D$, where D is the dielectric constant of the solvent medium according to

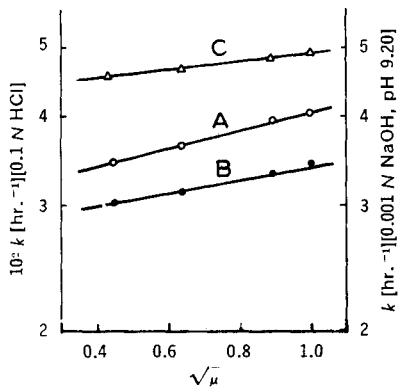

Figure 6—*Effect of ionic strength of the solvent medium on intrazole degradation in solution. Key: A, 0.1* N *HCl (65.0 ± 0.1°); B, pH 9.20 borate buffer (37.4 ± 0.1°); and C, 0.001* N *NaOH (30.0 ± 0.1°).*

Table III—Effect of Temperature on Rate Constants for the Degradation of Intrazole at Constant pH and Ionic Strength (0.5)

pH (Buffer)	Rate Constant × 10^2 hr.$^{-1}$ 65.0 ± 0.1°	75.0 ± 0.1°	85.0 ± 0.1°
0.1 *N* (HCl)	2.88	9.75	17.7
4.10 (Acetate)	0.352	0.725	1.97
	Rate Constant × 10 hr.$^{-1}$ 26.0 ± 0.1°	33.0 ± 0.1°	45.0 ± 0.1°
8.0 (Phosphate)	0.047	0.092	0.290
9.10 (Borate)	1.13	3.60	8.85
10.10 (Borate)	9.85	18.12	7.45

Eq. 9 as described by Scatchard (11):

$$\log k_{obs} = \log k_0 - \frac{NZ_A Z_B C^2}{2.303RT\, d_{AB}} \frac{1}{D} \qquad \text{(Eq. 9)}$$

where k_0 is the rate constant in a medium of infinite dielectric constant, and D is the dielectric constant of the solvent medium. Such a plot is shown in Fig. 7. The results show that as the dielectric of the medium is decreasing, the rate of hydrolysis of intrazole is also decreasing in acidic as well as in alkaline solutions. Thus, in acidic solutions the degradation of intrazole involves the attack of a positively charged hydronium ion on the uncharged intrazole molecule (10). In alkaline solutions the mechanism of degradation involves the attack of negatively charged hydroxide ion on the negatively charged intrazole anion. This will be discussed in detail in a later section on the mechanism of degradation.

Temperature Effects and Activation Energy—The temperature dependence of the hydrolysis of intrazole was determined by measuring the pseudo-first-order rate constant at various temperatures and hydrogen-ion concentrations at constant ionic strength (μ = 0.5). A list of the observed first-order rate constants under various conditions is given in Table III, and the corresponding Arrhenius-type plots are shown in Fig. 8. The heats of activation calculated from the slopes of the Arrhenius-type plots are: 19.8 kcal./mole in 0.1 *N* HCl, 21.4 kcal./mole at pH 4.10, and 20.3 kcal./mole at pH 8.00, 9.10, and 10.10. The heats of activation for the acid-catalyzed solvolysis of intrazole are within the range of 19–21 kcal./mole and agree well with the heats of activation for acid-catalyzed hydrolysis

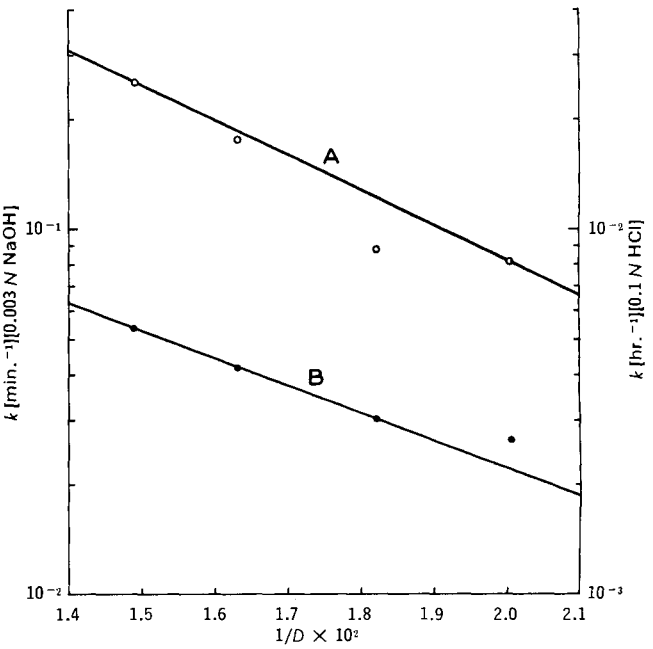

Figure 7—*Effect of dielectric constant of the solvent medium on the observed rate constant for intrazole degradation. Key: A, 0.1* N *HCl (65 ± 0.1°); and B, 0.003* N *NaOH (26 ± 0.1°).*

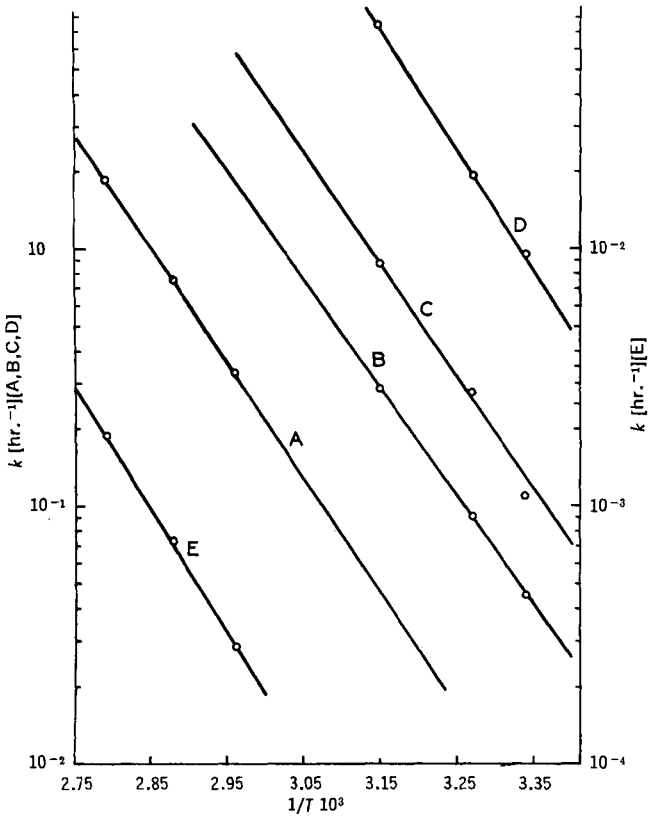

Figure 8—*Arrhenius-type plots showing temperature dependence of rates of hydrolysis of intrazole at various hydrogen-ion concentrations. Key: A, 0.1 N HCl; B, pH 8.00; C, pH 9.10; D, pH 10.10; and E, pH 4.10.*

of other monosubstituted and unsubstituted acyl amides (11). However, the disubstitution of the amide nitrogen leads to a much slower rate of hydrolysis in the acidic solutions.

The heats of activation for the alkaline hydrolysis of intrazole are also in the same range. However, in alkaline regions of pH 9.10 and 10.10, the heats of ionization of water are also included in ΔH_a values. The heat of ionization of water is 13.05 kcal./mole (12), which when substracted from 20.3 kcal./mole would result in 7.25 kcal./mole as the net heat of activation for the alkaline hydrolysis of intrazole.

Log Rate–pH Profile—Figure 9 shows the logarithm of the rate of degradation of intrazole under buffer-free conditions as a function of pH. In the pKa region the rate observed under buffer-free conditions cannot be explained by specific hydrogen- or hydroxyl-ion catalysis alone. To account for these excess rates in the intermediate pH range, the catalysis by solvent or spontaneous hydrolysis has to be implicated; a catenary that would explain the observed data, which is actually the sum of a number of terms, is shown in Eq. 10:

$$\frac{-d(\mathrm{INT})_T}{dt} = k_1[\mathrm{INTH}][\mathrm{H^+}] + k_2[\mathrm{INTH}] + k_3[\mathrm{INT^-}] + k_4[\mathrm{INT^-}][\mathrm{OH^-}] \quad \text{(Eq. 10)}$$

where [INTH] and [INT⁻] represent the concentrations of the neutral species and anion, respectively. The rate due to the attack of the solvent on unionized and ionized species of intrazole or spontaneous hydrolysis is represented by k_2 and k_3, respectively. Dividing both sides of Eq. 10 by the stoichiometric concentration of intrazole $(\mathrm{INT})_T$ gives Eq. 11:

$$\frac{d \ln (\mathrm{INT})_T}{dt} = k_{obs} = (k_1[\mathrm{H^+}] + k_2)f_{\mathrm{INTH}} + (k_3 + k_4[\mathrm{OH^-}])f_{\mathrm{INT^-}} \quad \text{(Eq. 11)}$$

At pH <2.0, intrazole exists virtually entirely as the unionized species (INTH), and the overall rate in this region may be attributed to terms in k_1 and k_2. From the values of k_{obs} in this region, k_1 was

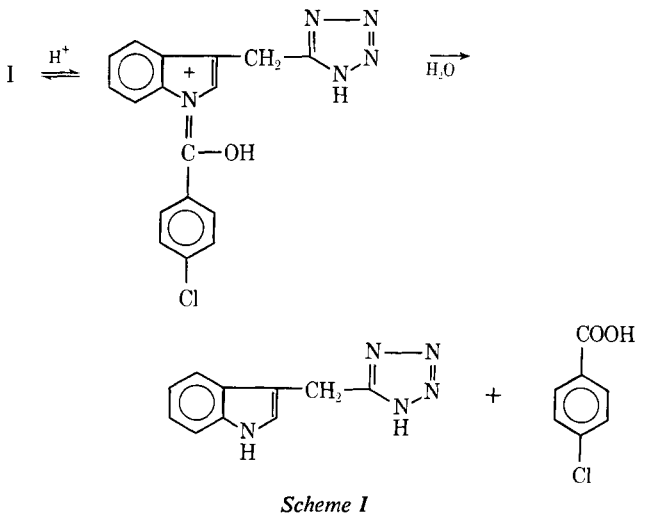

Scheme I

determined to be 0.361 l. mole^{-1} hr.$^{-1}$ and k_2 was determined to be approximately 2.2×10^{-3} l. mole^{-1} hr.$^{-1}$. At pH > 6.5, only terms containing k_3 and k_4 contribute to the overall rate; from these data, k_3 was found to be 5.0×10^{-3} l. mole^{-1} hr.$^{-1}$ and k_4 was found to be 5.37×10^{-4} l. mole^{-1} hr.$^{-1}$. The value of k_w used here was 1.212×10^{-13} extrapolated from data of Harned and Hammer (13). Further verification of the values of k_2 and k_3 comes from the middle portion of the profile where only the terms in k_2 and k_3 contribute.

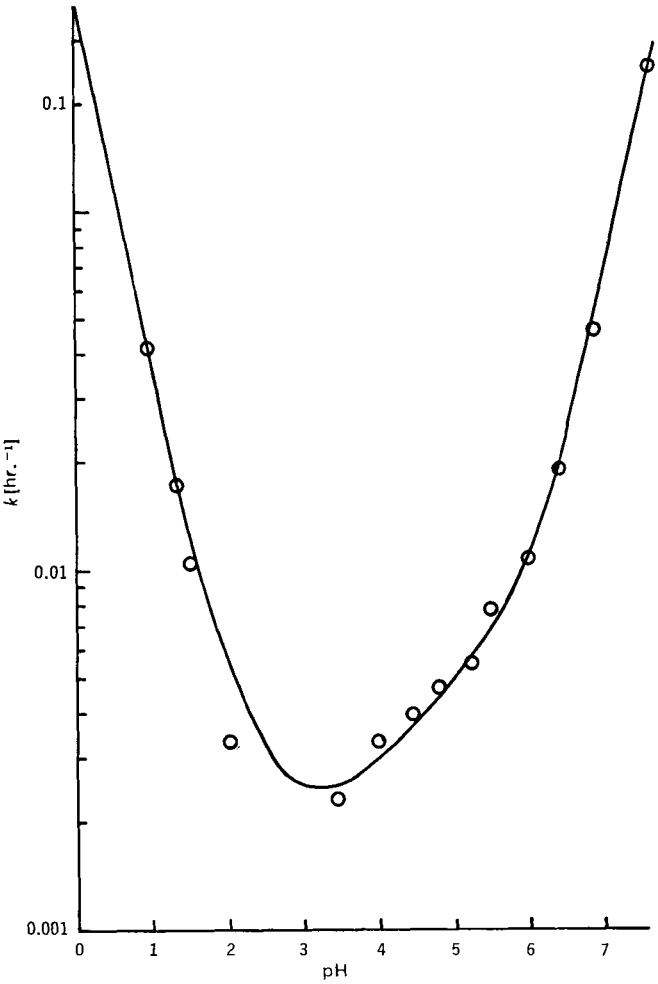

Figure 9—*pH–log rate profile of intrazole degradation in solution at constant pH and 65° (μ = 0.5). The curve represents the theoretical line calculated from the rate constants, while the points are experimental results.*

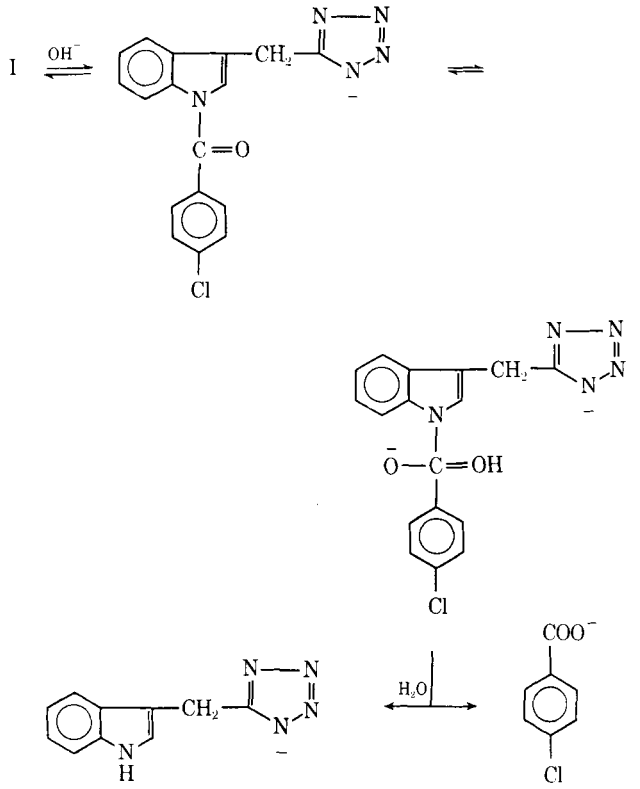

Scheme II

The curve in Fig. 9 was calculated from these constants, while the points are experimental results. The model shown in Eq. 11 was used to calculate the average kinetic pKa and was found to be about 4.5, whereas the experimentally determined pKa is 4.4 which satisfies the choice of this kinetic model. It is particularly interesting to note the relatively rapid rate of hydrolysis of intrazole in neutral solution compared to other amides.

From the curve, it can be seen that the pH of the minimum degradation rate is about 3, and this would be the optimum pH for formulation of a liquid product.

Mechanism of Intrazole Degradation—In the acid-catalyzed degradation of intrazole, only two products were identified by TLC. These two products were *p*-chlorobenzoic acid and 3-(5-tetrazolylmethyl)indole. These two products accounted for about 95% of the material spotted on the TLC plate. However, it was found that with pure materials (reference compounds) the recovery was only 92–95%. Consistent with the products formed from the hydrolysis, the mechanism for the degradation of intrazole in acidic media can be written as shown in Scheme I.

This mechanism is supported by the primary salt effect on the rate of hydrolysis of intrazole under acidic conditions. The mechanism is further substantiated by the effect of ethanol on the rate of hydrolysis of intrazole in acidic solutions. As the dielectric constant of the medium decreased (that is, as the alcohol concentration increased), the rate of hydrolysis also decreased, thereby indicating that the rate-determining step involved the attack of hydronium ion on a neutral species.

In alkaline solutions also, the products of hydrolysis were *p*-chlorobenzoic acid (as the anion) and 3-(5-tetrazolylmethyl)indole. The mechanism of hydrolysis can be written as shown in Scheme II. Supporting evidence for this mechanism is the positive primary salt effect on the hydrolysis of intrazole in alkaline solutions. The rate of hydrolysis increased with increasing ionic strength in the hydrolytic medium, indicating that the negatively charged hydroxyl ion attacked the anion of intrazole in the rate-determining step. A further piece of evidence in support of this hypothesis was the decrease in the rate of hydrolysis in alkaline solutions as the dielectric constant of the hydrolytic medium was decreased. Staab (4) showed that in the series *N*-acetylindole, *N*-acetylbenzimidazole, and *N*-acetylbenzotriazole the $t_{1/2}$ for hydrolysis at 25° at pH 7.0 in water was ∞, 760, and 115 min., respectively. The increase in the hydrolytic rate of *N*-acetylbenzotriazole over that of the other two derivatives was attributed to the reactivity of the benzotriazole moiety and the delocalization of the electrons on the carbonyl oxygen. However, $t_{1/2}$ calculated for the hydrolysis of intrazole at pH 7.20 and 25° was 270 hr. Thus, the increased reactivity of carbonyl of intrazole over that of *N*-acetylindole can be attributed to the electron-withdrawing nature of the *p*-chlorobenzoyl group resulting in weakening of the amide bond.

REFERENCES

(1) J. S. Fleming, M. E. Bierwagen, A. W. Pircio, and M. H. Pindell, *Arch. Int. Pharmacodyn. Ther.*, **178**, 423(1969).

(2) P. F. Juby and T. W. Hudyma, *J. Med. Chem.*, **12**, 396(1969).

(3) H. A. Staab, *Chem. Ber.*, **89**, 1929(1956).

(4) *Ibid.*, **90**, 1320(1957).

(5) R. M. C. Dawson and W. H. Elliott, in "Biochemist's Handbook," C. Long, Ed., E. & F. N. Spon Ltd., London, England, 1961, p. 19.

(6) C. W. Davies, "Ion Association," Butterworths, Washington, D. C., 1962, p. 97.

(7) K. A. Connors, "Textbook of Pharmaceutical Analysis," Wiley, New York, N. Y., 1967, p. 26.

(8) F. R. Benson, "Heterocyclic Compounds," Wiley, New York, N. Y., 1967, p. 9.

(9) E. R. Garrett, *J. Pharm. Sci.*, **51**, 819(1962).

(10) K. J. Laidler, "The Chemical Kinetics of Enzyme Action," Oxford University Press, London, England, 1958, p. 47.

(11) G. Scatchard, *Chem. Rev.*, **10**, 229(1932).

(12) E. R. Garrett and D. J. Weber, *J. Pharm. Sci.*, **51**, 387(1962).

(13) H. S. Harned and W. J. Hammer, *J. Amer. Chem. Soc.*, **55**, 2194(1933).

ACKNOWLEDGMENTS AND ADDRESSES

Received January 24, 1972, from *Product Development Research, Bristol Laboratories, Syracuse, NY 13201*

Accepted for publication May 17, 1972.

Presented to the Basic Pharmaceutics Section, APhA Academy of Pharmaceutical Sciences, Houston meeting, April 1972.

The authors thank Mrs. V. H. Silver for her excellent technical assistance and Dr. W. H. Johns and Dr. M. A. Schwartz for helpful suggestions.

▲ To whom inquiries should be directed.